THE ASTROPHYSICAL JOURNAL, 332:26–43, 1988 September 1

GALAXY FORMATION AND CLUSTERING IN AN *N*-BODY EXPERIMENT

R. G. CARLBERG
Department of Astronomy, University of Toronto
Received 1987 October 30; accepted 1988 March 1

ABSTRACT

The formation of galaxies and their clustering is studied with an N-body model augmented to include a simple description of gas cooling and star formation. The gas particles in the model mimic the basic features of atomic cooling; that is, at low densities and high temperatures the gas is nearly adiabatic, but at higher densities and lower temperatures it cools effectively, and at very high densities, the gas converts into stars. The critical densities and temperatures for cooling and star formation are based on the radiative cooling curve. Two experiments are presented: an $\Omega = 1$ model and an $\Omega_i = 5/3$ "cluster" model, both with perturbations drawn from a density perturbation spectrum with $n = -1$. The galaxies form with an enhanced clustering with respect to the underlying dark matter distribution, that is, the galaxies prefer to form in especially overdense regions of the initial density fluctuation field. As a consequence, the correlation function evolves more slowly with redshift than in the dark matter distribution. Mergers occur preferentially between galaxies in densely clustered environments, leading to a buildup of a correlation between initial overdensity and mass of the galaxy. Star formation is spread over the time interval during which galaxies can freely accrete gas-rich material, and the stellar mass of an average galaxy in the experiment increases by 36% from a redshift of 0.56. In contrast, star formation in the "cluster" experiment is abruptly terminated as the hot, nearly adiabatic, cluster gas sweeps remaining halo gas from the galaxies. The total mass in gas in the cluster is twice the mass in cluster galaxies. The gas temperature profile appears to be very nearly isothermal. Besides the gas and dark matter, the cluster contains a substantial smoothed out distribution of stars that are stripped off the galaxies by tidal fields.

Subject headings: cosmology — galaxies: clustering — galaxies: formation

I. INTRODUCTION

The relation between galaxies and the dominant dark matter distribution is unlikely to be straightforward, since the formation of visible galaxies is both dissipative and subject to strong influence from the cosmological environment that tends to segregate the eventual stellar component from the dark matter. That is, after a high-density region turns around from the universal expansion, infall and mergers may continue to build up to galaxy, and stripping may remove gas (Gott and Gunn 1972; Gunn 1977; Toomre 1977). Aside from the problem of understanding the structure of galaxies, these interactions lead to complications in attempts to measure the large-scale properties of the universe, since both the numbers, luminosities, and sizes of galaxies change with redshift, and the galaxies are unlikely to be a fair tracer of the dark matter. A previous paper (Carlberg 1988, hereafter Paper I) presented a numerical experiment containing two components, collisionless dark matter and an isothermal gas, that was a first step toward introducing a dissipative component that more realistically models galaxies than the collisionless dark matter alone. That model is now extended to include a star formation algorithm that turns gas particles into star particles and to improve the treatment of cooling in the gas.

This paper aims to show that the galaxies formed in these experiments are similar in many aspects to galaxies observed in the universe, at least in their gross global properties. Two properties of the galaxies are emphasized. First, their formation time is spread over the long interval during which they can freely accrete gas and galaxies from the surrounding medium. And second, even though the galaxies in the experiments form in such a way that they are not an unbiased tracer of the bulk of the mass in the experiment, they do leave observable clues to their relative degree of biasing.

The next section gives the details of the gas cooling and star formation algorithm, and the motivation for the choice of parameters in the model. Section III describes the rate of formation of the stars and galaxies and their relation to peaks in the initial density distribution. The distribution of the contents of the cluster is described in § IV.

II. NUMERICAL METHODS

a) Initial Conditions and Gravitational Forces

The numerical code uses the same basic methods as in Paper I. The experiment begins with 32,768 gas particles and 32,768 dark matter particles placed in a periodic cube having edges 64 units long. The gas particles, each weighing 1/10 of a dark particle, initially sit on top of their dark particle partners. The particles are created with a uniform random number generator and then perturbed with the $P(k) \propto k^{-1}$ spectrum and given appropriate velocities. The relatively small number of particles used here, effectively 32,768, means that the $n = -1$ spectrum drops into the white noise around half the Nyquist frequency. Consequently most of the nonlinear structure appears to grow from a $n = 0$ spectrum, although the bias that develops is aided by the $n = -1$ power on long wavelengths. The particle perturbations required to realize the spectrum are calculated using a modified version of the acceleration calculation. The density perturbation spectrum is assigned to the grid with random phases and amplitudes fixed at the values specified by the spectrum. This spectrum is then multiplied by the Green's Function for the potential, inverse transformed, and then differentiated to give the perturbations in positions. The Zeldovich approximation gives the initial growing model peculiar velocities as the displacement multiplied by the Hubble rate of expansion (for $\Omega = 1$).

Two experiments are performed. The first is designed to study a small region that ultimately turns into a group of galaxies and is a direct extension of the experiment presented in Paper I. The comoving coordinate system moves in a cycloid, expanding 2.5 times to a maximum at $t = \pi$, then rather than being allowed to recollapse, the grid is help fixed and run on to $t = 10.39$. The initial Ω is 5/3. Holding the grid fixed has the benefit of maintaining resolution as the cluster develops. The main drawback is that accretion from the surrounding medium is diminished, and a lesser problem is that the images of the cluster cause unrealistic tides. The dwindling of accretion toward the end of the experiment decreases gravitational heating of the cluster, and in as much as the individual galaxies survive merging this experiment somewhat overemphasizes the "overmerging" problem in a cluster. Overall, the experiment should be a representative model of a relatively isolated cluster and not unduly compromised by the nature of the grid.

The second experiment is a standard $\Omega = 1$ model; it is intended to model a representative segment of the universe and can be compared to the dense environment of the first model. The current epoch is identified as the experiment after an expansion by a factor of 10.9, reached at time 35.8, although the experiment is run on to time 81.3.

The gravitational forces are calculated with a PPPM code that can resolve gravity over three decades of length scales. In Paper I the Green's function on the mesh was symmetrized for a single particle half a box away to reduce tidal forces. Here the image charges are explicitly added in the Green's function. The potential of a single particle then has a maximum half a cube edge away in the three principal directions. Consequently, particles at large radii take longer to fall into the cluster, and they arrive with slightly less energy than in the calculations of Paper I, comparison showing that the time scale of events at late times is increased by $\sim 10\%$.

The time step is set to 0.05 of the current age of the experiment, to a maximum of 0.35 units. Initial experiments that used time steps of 0.02 of the age gave essentially identical results, at 2.5 times the cost. The softening length in the $\Omega_i = 5/3$ experiment is set to 0.25 of a grid unit, and kept fixed at that value. In the $\Omega = 1$ model the softening length begins as 1 grid unit but then maintains that physical length as the experiment expands. This softening is later scaled into a physical length of $\sim 50h^{-1}$ kpc.

b) *Gas and Star Particles*

The numerical description of gas and star formation is a deliberate simplification of the radiative cooling curve (Rees and Ostriker 1977; Silk 1977; Blumenthal *et al.* 1984). Cooling and star formation are implemented by treating the gas particles as "superatoms"; that is, literally translating atomic collision processes into corresponding collisions in the code. The advantages of the proposed scheme are ease of implementation, high speed of execution, low storage overhead, and physical properties that are easily calculated from standard kinetic theory. In the limit that the number of particles is very large this scheme does converge to the behavior of a normal gas, but it is not a universal gas dynamics algorithm. It is specifically designed to be useful for gas dynamics within "galaxies" containing relatively few gas particles. The main drawback is that the results are noisier than a particle smoothing scheme would give, although the galaxies here have sufficiently few particles that it is not clear that smoothing would lead to any significant improvement.

Candidate pairs of particles for collision are found by dividing the cube into subboxes (randomly shifted each time) such that on the average every subbox contains a few particles, although dense regions have several hundred particles in a box. The particles in the subbox are paired with the nearest approaching particle, thus boxes will often have one unmatched particle. The collision scheme is invoked every second time step, since typical gas particle velocities will usually take several steps to travel one subbox. Furthermore, increasing the collision frequency increases the numerical viscosity from particle collisions.

The outcome of a collision depends on the local density and temperature and a simplified version of the radiative cooling curve (Raymond, Cox, and Smith 1976). The features of the cooling curve relevant to galaxies are that galactic masses and sizes have inferred cooling times less than a free-fall time, whereas larger gas masses, such as groups of galaxies, take longer to cool. A series of preliminary experiments clearly revealed that galaxies as distinct stellar objects only develop for a relatively narrow range of conditions. Radically changing the density and temperatures for cooling and star formation has two most likely outcomes: either nearly complete early star formation resulting in stars distributed rather like the dark matter, or at the other extreme, no stars at all, only hot gas, once again distributed like the dark matter.

Cooling and star formation depend on the local density and temperature. Once a pair is selected to collide, the density is estimated from the particle pair's co-moving relative separation, Δr, as $\rho = \bar{\rho}(t)\Omega_b/(l/\Delta r)^3$, where $\bar{\rho}(t)$ is the mean mass density at time t, Ω_b is the baryonic fraction, and l is the mean separation of the baryons. The local temperature is related to the co-moving relative velocity along the line of centers, Δv, as $T = [a(t)C\,\Delta v]^2/R$, where $a(t)$ is the expansion factor, C is a scaling constant that is determined by the physical size of the experiment, and R is the gas constant.

It was considered undesirable and probably unrealistic to follow the details of the lowering of the temperature in a shocked gas, at least in these initial experiments. The cooling is therefore simplified to abrupt transition boundaries in temperature and density, and the consequences of a collision are separated into three possibilities: (1) adiabatic collisions at low densities or high temperatures, (2) instantaneous cooling given both sufficient density and a low enough temperature, and (3) conversion of gas particles to collisionless star particles at very high densities. In detail this works as follows. High temperature, low-density gas should be adiabatic if the temperature exceeds $T_{\rm cool}$ or the density is less than $n_{\rm cool}$. Adiabatic collisions are realized by reversing the relative velocities about the line of centers of the colliding particles. The boundary between cooling and no cooling is somewhat blurred, since gas whose temperature exceeds the cooling threshold will have some members of the population at low relative velocities that will lead to cooling collisions. If the particles meet the criteria too cool, the particles' postcollision velocities are lowered as in Paper I; that is, the particles are brought to their center of mass and momentum and assigned velocities drawn from a Maxwellian distribution of a lower temperature.

This algorithm for gas cooling yields cool gas that sinks deep within galactic size potential wells and then soon turns into stars, leaving hot, low-density gas in larger dark halos. The transport properties, viscosity and heat conduction, of the hot gas can be simply and reliably calculated from first principles.

To set the values of the critical densities and temperatures the $t_{ff} = t_{cool}$ diagram of Blumenthal *et al.* (1984) is used as a guide. Cooling is ineffective in a free-fall time for mean gas densities less than $\sim 10^{-4}$ cm^{-3} and temperatures greater than 1×10^7 K. Stellar galaxies have mean densities greater than 10^{-2} cm^{-3}. The actual critical densities and temperatures used depend on a combination of the physical scaling of the experiments and numerical convenience. The collision algorithm works directly with the relative co-moving separation, Δr, and relative co-moving velocity, Δv, of the colliding particles. For the $\Omega_i = 5/3$ experiment the critical density required for cooling was set at 1.3×10^{-5} cm^{-3} and for star formation of 1.0×10^{-1} cm^{-3}, equivalent to $d_{cool} = 1/a(t)$, and $d_* = 0.05/a(t)$, where $a(t)$ is the expansion factor, equal to 1 at maximum expansion. The cooling temperature is set using the result from Paper I that the one-dimensional velocity dispersion of the cluster that forms will be ~ 12 velocity units at the end of the experiment. Equating this to the velocity dispersion of a typical group, 500 km s^{-1}, translates the critical relative co-moving velocity for cooling into $6/a(t)$ velocity units.

To obtain physical density and temperatures in the $\Omega = 1$ experiment requires that its initial redshift and size be specified. Based on a preliminary experiment, it was decided that experiment should be expanded by a factor of ~ 10 and the box size was around 40 Mpc. The critical density for cooling is set at 2.9×10^{-4} cm^{-3}, or $d_{cool} = 2/a(t)$ units and the density for star formation is 1.8×10^{-2} cm^{-3}. or $d_* = 0.25/a(t)$ unit. Upon cooling the gas temperature is instantly reduced to 4×10^4 K, equivalent to $0.4/a(t)$ velocity units. The cooling velocity is set at $v_{cool} = 1/a(t)$ units.

III. GALAXY FORMATION

a) Galaxy Evolution

The experiments begin as a mixture of cold gas and dark matter. Snapshots of their evolution are shown in Figure 1, for $\Omega_i = 5/3$, and Figure 2, for $\Omega = 1$. The figures show separate *x-y* and *x-z* projections for each type of particle, i.e., gas, star, and dark matter. The basic features of the experiments are straightforward, the main difference from a normal collisionless *N*-body experiment is that the dense gas at the bottom of the potential wells turns into stars. The dark halos around galaxies remain loaded with considerable amounts of gas that continues to fuel star formation and a gradual growth of the galaxies. Besides this gentle inflow of gas from a galaxy's own halo, the protogalaxies merge to build up more massive galaxies.

In the "cluster" experiment the velocity dispersion in the cluster gradually rises as the halos surrounding the galaxies merge. The galaxies eventually have most of the outer parts of their dark halos stripped off and are then free to orbit with relatively little dynamical friction, as in Paper I. As the cluster grows, the remaining gas in the halos merges, and the gas temperature is raised to the same internal random velocity as the velocity dispersion of the dark matter in the cluster, although the gas has a nearly isotropic velocity ellipsoid. As the velocity dispersion rises the gas becomes hot enough that it can no longer cool. Subsequently, the galaxies in the cluster consume their remaining dense, cool gas, and star formation more or less ceases. This experiment is stopped at time 10.39, with most of the galaxies in two groups, the smaller one destined to fall into the larger one. As discussed in Paper I the galaxies are unlikely to merge or suffer significant dynamical friction beyond this time, partly because the galaxies are relatively light, and partly because continuing infall pumps energy into the orbits of the galaxies.

The formation of groups of galaxies seen in this experiment emphasizes the dynamic nature of the process, particularly that a protocluster is clearly present at the time that the galaxies are subject to the greatest tides and most likely to merge (Merritt 1984). Thereafter clusters attract a continuing infall of dark matter and galaxies that brings in "fresh" galaxies. As the cluster in Figure 1 grows the gas distribution spreads out smoothly from the individual galaxies. Note that the gas distribution is considerably smoother than the underlying dark matter distribution. That is, the X-rays that the hot gas emit will give a smoothed impression of the lumpiness of the dark matter that dominates the potential. Clusters that have very smooth X-ray emission, such as Coma, may be dynamically less relaxed than the hot gas would lead one to believe (see also Fitchett and Webster 1987).

b) Galaxy Properties and Scaling

Dense groups of stars that are identified as galaxies are found by linking together all particles closer than some minimum distance. Ideally one would choose the link length so that the identified objects would scale to the size of observed galaxies, typically $5h^{-1}$ kpc for a standard bright galaxy. For the $\Omega = 1$ experiment this is a very demanding criterion, since the correlation length, at $5h^{-1}$ Mpc, is 1000 times longer than the galaxy length scale. Unfortunately the softening length scales to a value 10 times larger than the physical sizes of galaxies, so the galaxies identified in the $\Omega = 1$ experiment are rather fluffy, although for many purposes the sizes of the galaxies is irrelevant.

The sizes and masses of objects found in the $\Omega = 1$ experiment using different linking lengths are displayed in Table 1, imposing a minimum galaxy mass cutoff at 10 particles. Of the 16,546 star particles present at $t = 35.8$, the adopted linking length of 0.2 grid units binds all but 1379 with neighbors. The mean overdensity of an average galaxy at the average radius is 5.8×10^4. Shorter linking lengths tend to find the cores of the galaxies already identified by the longer linking lengths, so that the correlation properties of the objects found at shorter linking lengths are essentially unchanged.

An *x-y* projection of the galaxies identified in the $\Omega = 1$ model, using their half mass radii for the box sizes, is shown in Figure 3. Clearly, the dot plots of Figures 1 and 2 fail to show the discrete and distinct nature of the objects identified as galaxies. About two-thirds of the stars are in galaxies, the rest

TABLE 1

GALAXY FINDING

Link Length	N	$\langle r_h \rangle$	$\langle m \rangle$
0.01	10	0.008	16
0.02	48	0.020	18
0.03	95	0.032	25
0.05	148	0.049	32
0.10	210	0.075	38
0.20	243	0.112	43
0.30	241	0.137	48
0.50	240	0.184	52

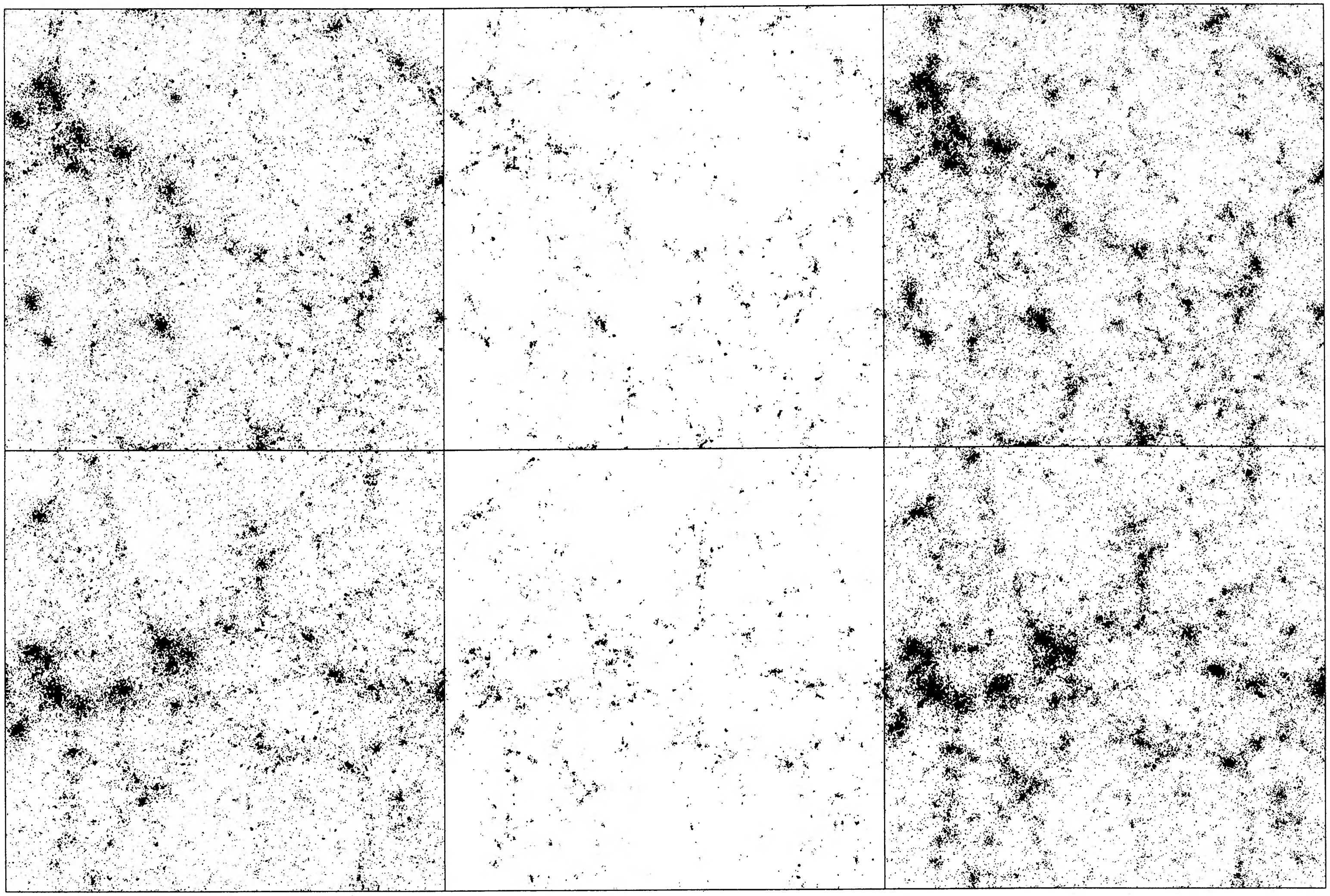

FIG. 1*a*

FIG. 1.—The *x-y* (*top row*) and *x-z* (*bottom row*) projections of the gas (*left*), star (*middle*) and dark matter particles (*right*) in the $\Omega_i = 5/3$ cluster simulation at times (*a*) 2.39, (*b*) 6.39, and (*c*) 10.39. The box scales to 2.56 Mpc on a side.

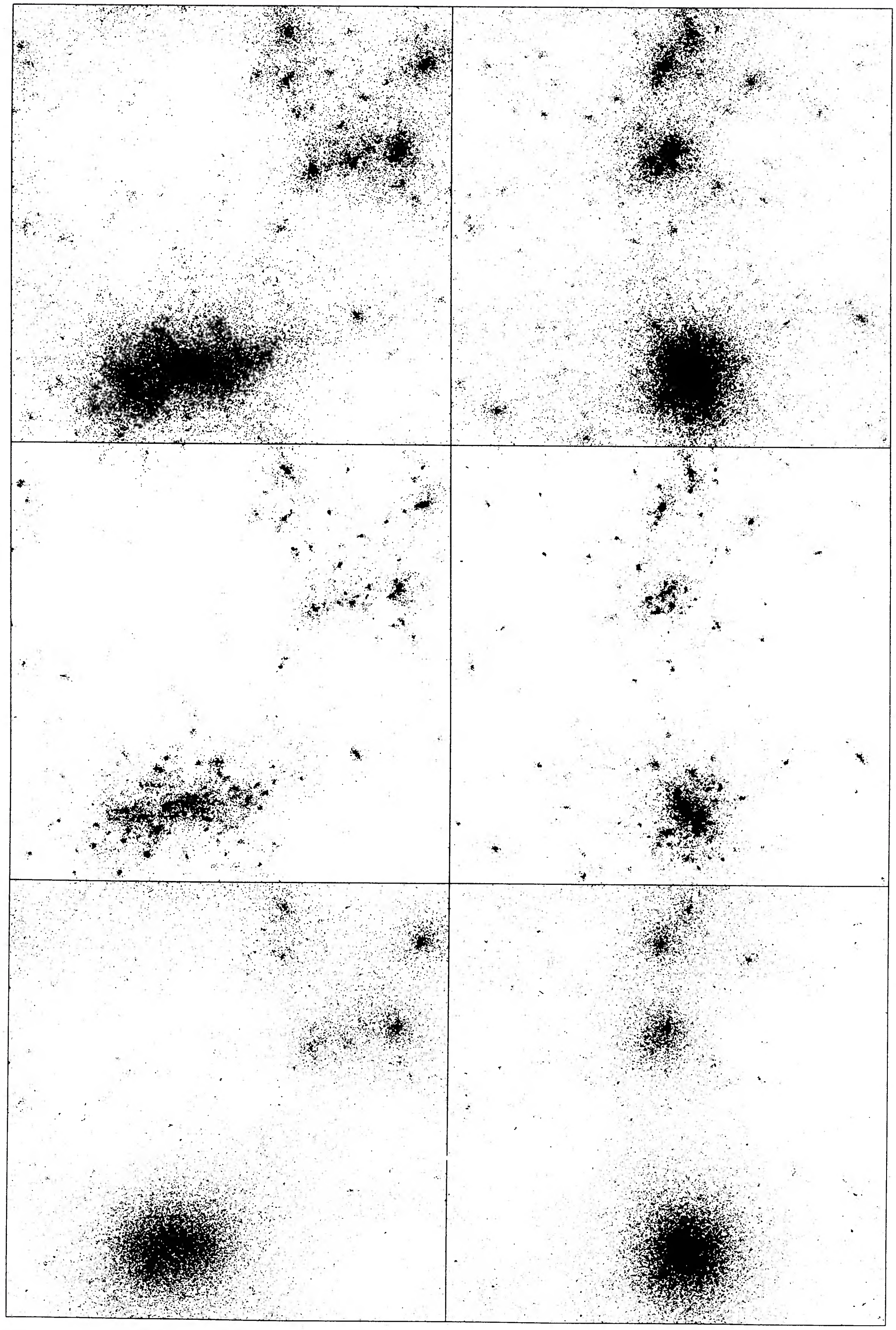

FIG. 1b

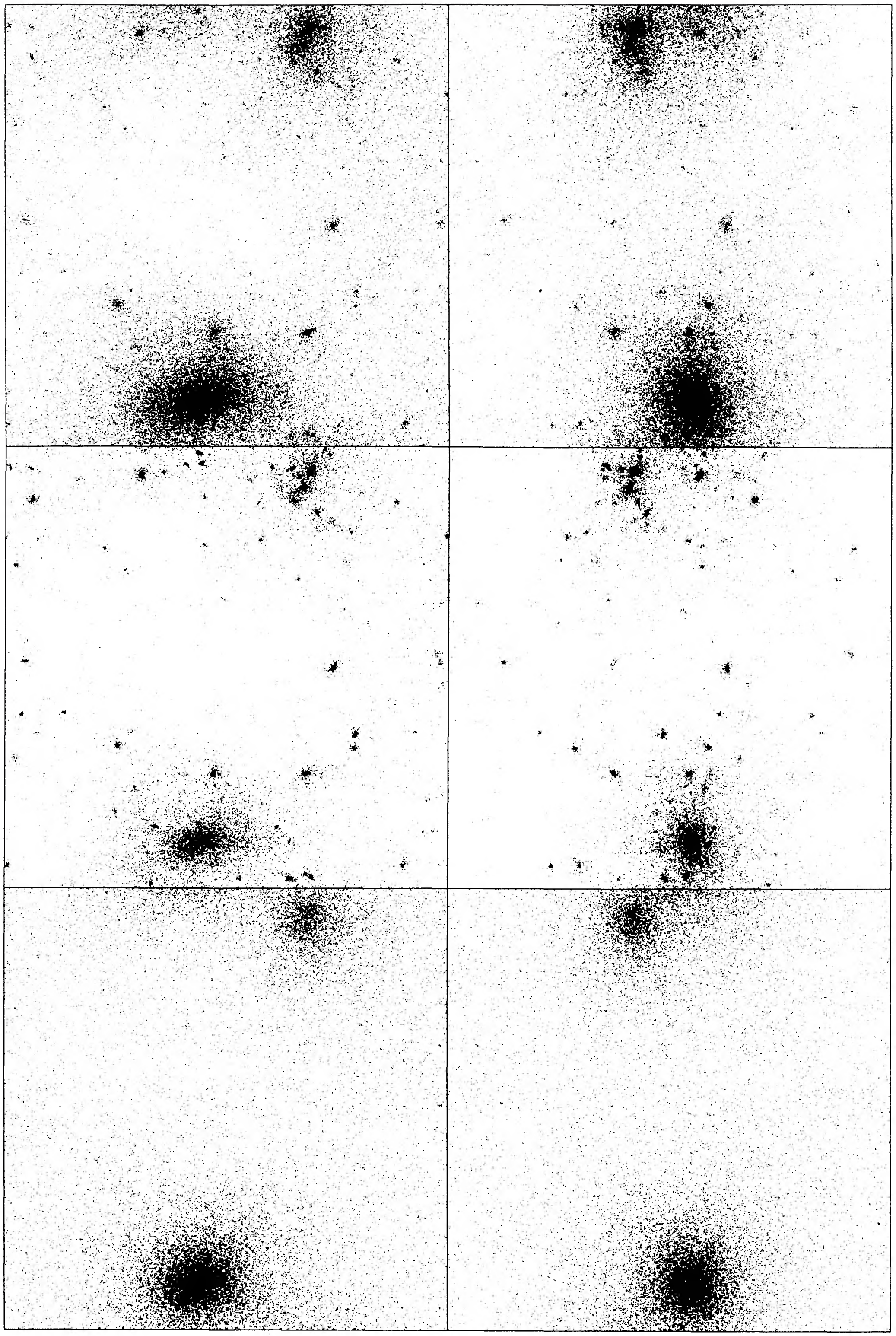

FIG. 1c

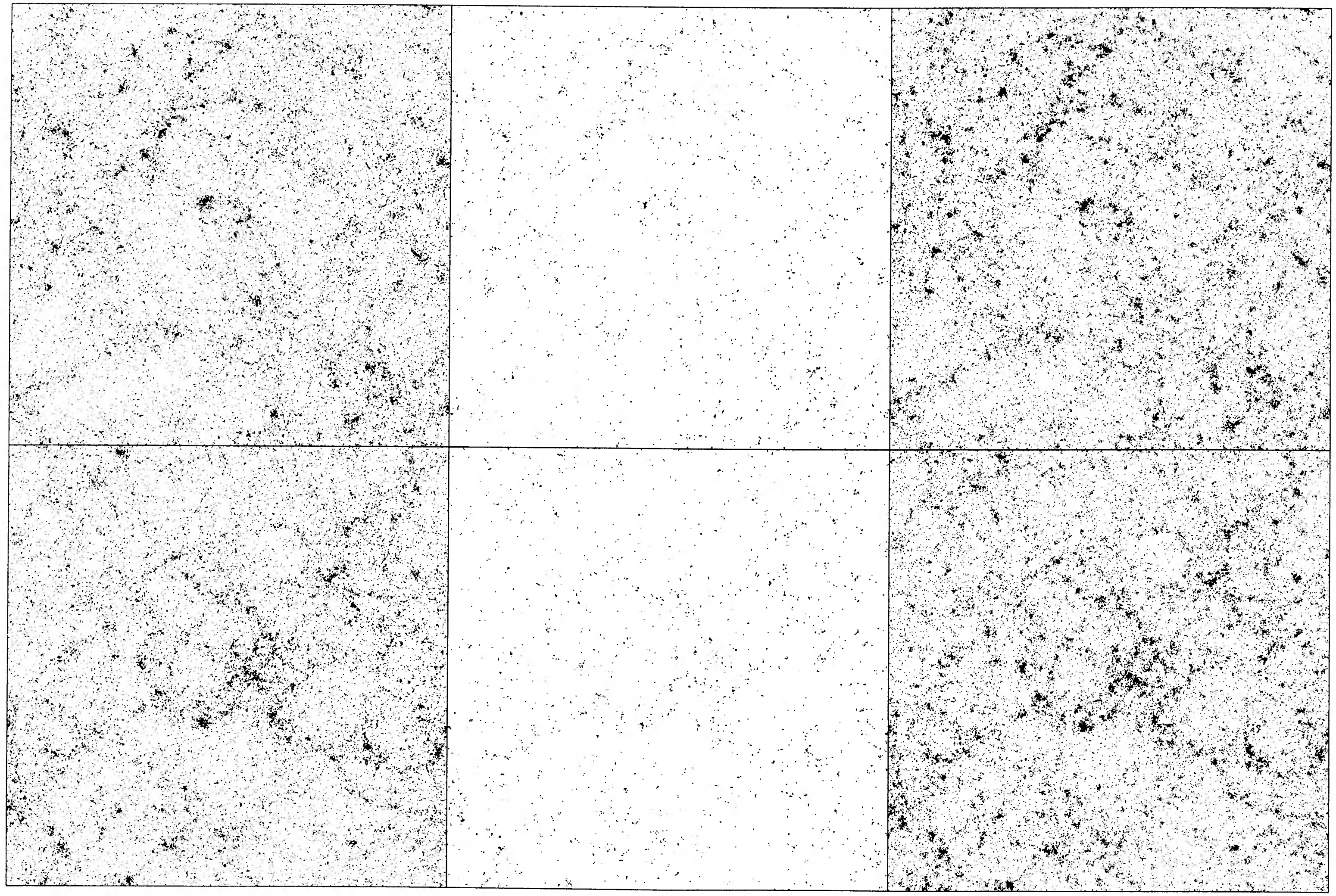

FIG. 2.—The *x-y* (*top row*) and *x-z* (*bottom row*) projections of the gas (*left*), star (*middle*) and dark matter particles (*right*) in the $\Omega = 1$ experiment at times (*a*) 5.96 and (*b*) 35.8. The box is $40h^{-1}$ Mpc on a side.

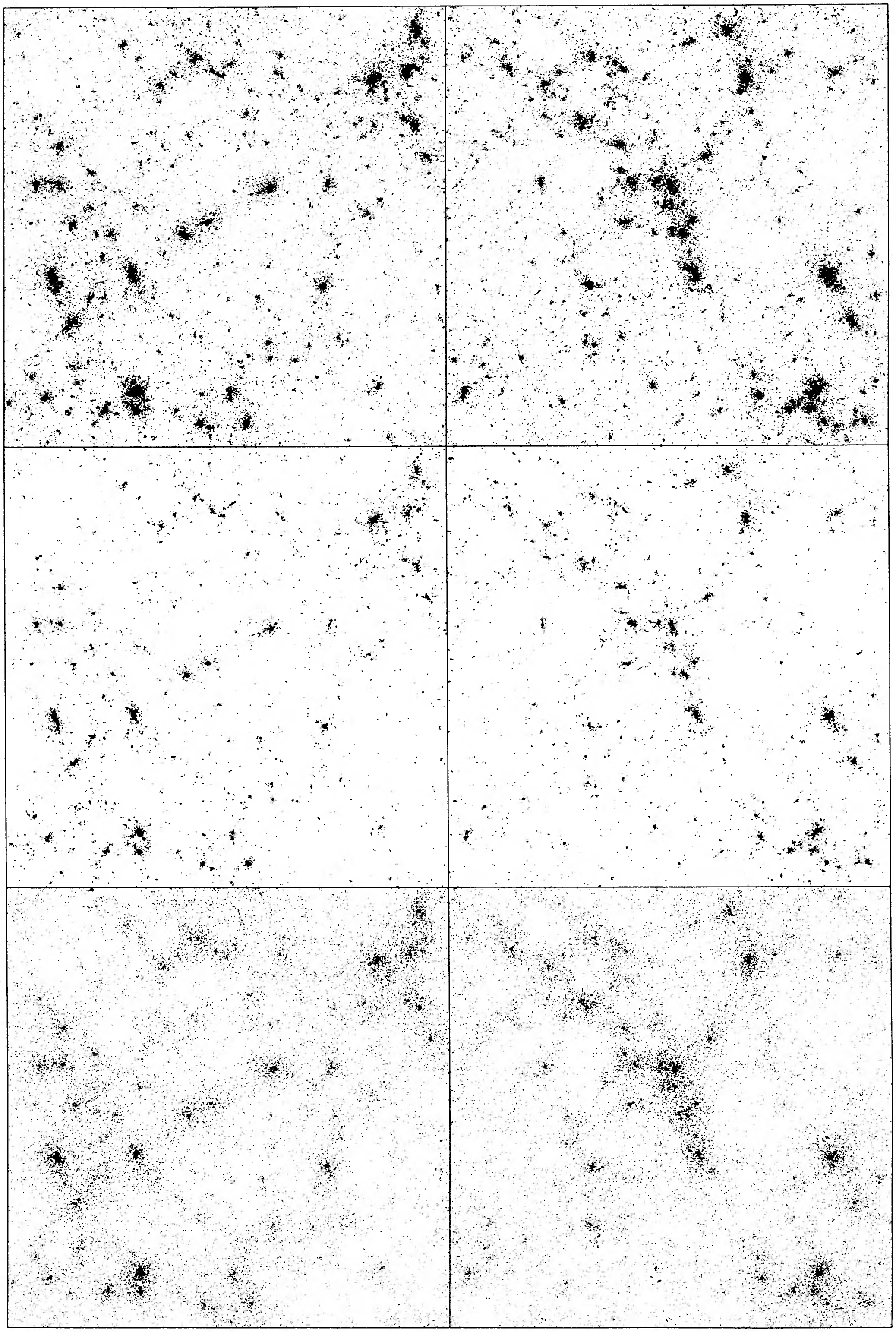

FIG. 2b

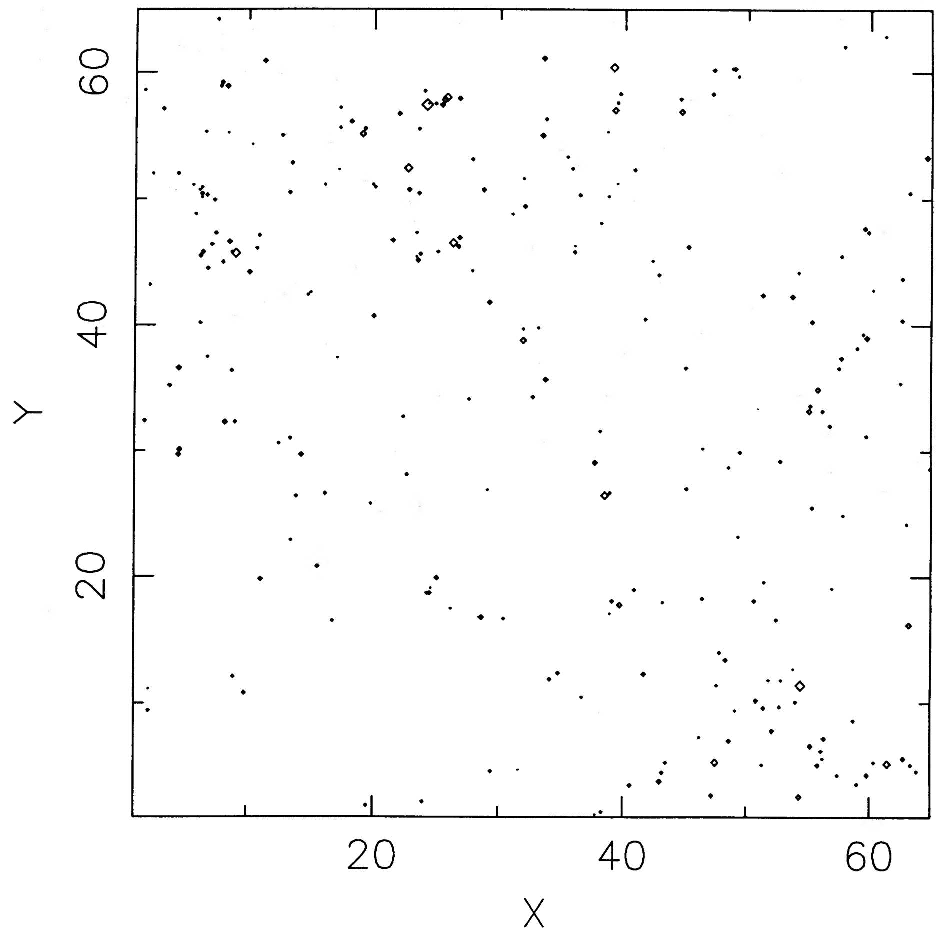

FIG. 3.—The x-y projection of the galaxies identified in the $\Omega = 1$ experiment at time 35.8, where the diagonal of the box is equal to the half mass diameter of the galaxy.

are floating around loose in groups, most near the edges of the galaxies.

At the final moment of the $\Omega = 1$ experiment the correlation length is measured to be 8 grid units. Equating this to a correlation length of $5h^{-1}$ Mpc (Davis and Peebles 1983) yields a physical scaling of the sizes in the experiment. The entire box of 64 grid units is $40h^{-1}$ Mpc on a side, and the mean radius of the galaxies, at 0.112 grid units, scales to $70h^{-1}$ kpc. The Hubble velocity across the box is 0.149 units, thus the velocity unit is 3356 km s^{-1}. The one-dimensional peculiar velocity dispersion of the galaxies is 0.118 units, scaling to 396 km s^{-1}, similar to the value inferred from observations by Davis and Peebles (1983) and Bean *et al.* (1983).

A problem is evident when one scales to the mass of the galaxies. The mass of a single gas particle works out to 4.9 $\times$ $10^{10}h^{-1}(11\Omega_b)\ M_\odot$. This very large mass per particle means that average galaxy mass is $2 \times 10^{12}\ M_\odot$ of baryons, excessively large. The sizes and masses of the galaxies in the experiment are larger than real galaxies, so in as much as galaxy evolution depends on the details of the galaxies, rather than the distribution and motion of the surrounding dark matter the results found here must be viewed with some caution. The basic problem is that there are relatively few particles in a relatively large box. A future paper will discuss a box of half the size containing 8 times as many particles.

The mass-radius relation of the objects identified as galaxies is shown in Figure 4. At the current epoch the softening length has been reduced to 0.092 units, so most of the objects are partially resolved, although they have so few particles that nothing reliable can be said about their internal structure.

In the cluster experiment a different approach is chosen for scaling. The average internal one-dimensional velocity dispersion of the stars in the galaxies at $t = 10.39$ is 4.3 units. If this is equated to an average one-dimensional velocity dispersion of 200 km s^{-1}, then the cluster velocity dispersion of 11 units scales to 511 km s^{-1}, a reasonable value for a group of galaxies (Huchra and Geller 1983). The sizes of the objects at the final moment averages 0.25 units, and the half mass radius of the larger group is near to 5 units, a ratio of 20. If galaxies have half mass radii of 10 kpc, this would imply a group half mass radius of 200 kpc, a bit on the small size, but not out of the observed range. The adopted length scaling of 40 kpc per grid unit implies a box size of 2.56 Mpc. A mass scaling is established by taking the mean density in the volume to be equal to $9\pi^2/16$ times the current critical density implying a mass per star particle of $7.2 \times 10^7 h^2\ M_\odot$. The average galaxy then has a stellar mass of $5.1 \times 10^9\ M_\odot$, equivalent to a luminosity of $M_B = -18.9$, if $M/L = 1$.

c) Star Formation Rate

The star formation rates for the cluster model and the $\Omega = 1$ model are shown in Figures 5 and 6, respectively. The

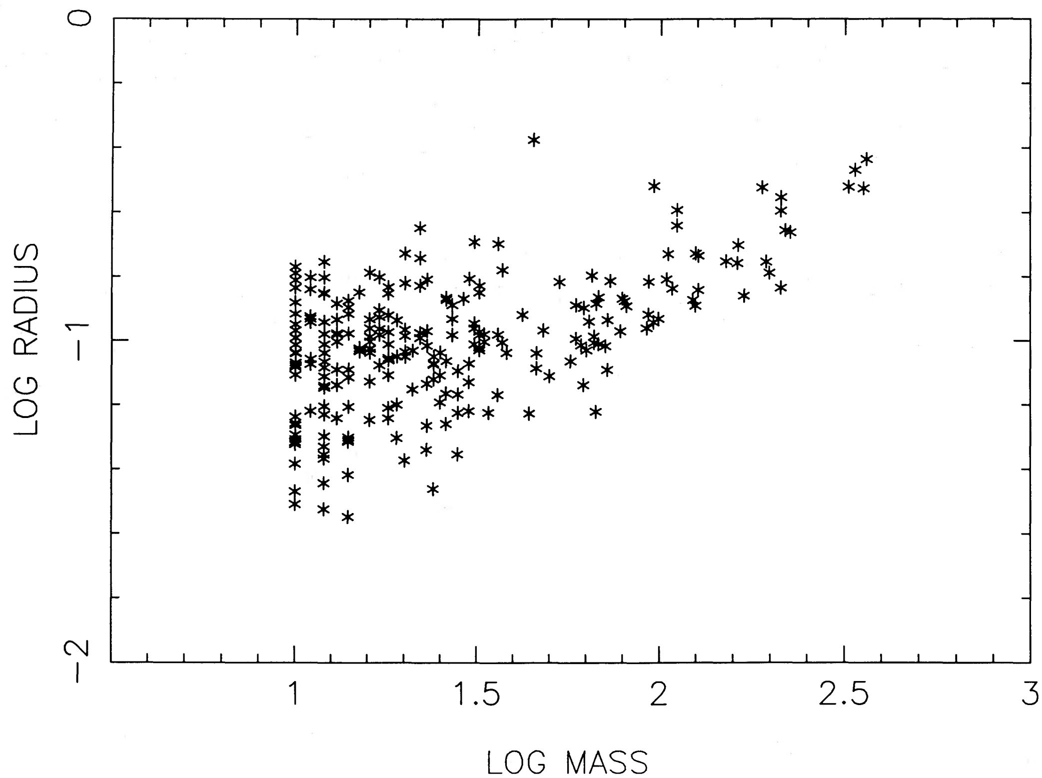

FIG. 4.—The mass-radius diagram, both as logarithms, of the identified galaxies in the $\Omega = 1$ experiment at time 35.8. The radii are measured in grid units. At this time the correlation length is nearly 10 units. The softening length remains constant in physical units and is equal to 0.09 at this time, so that the galaxies are partially resolved. The $\Omega_i = 5/3$ experiment has galaxies that are typically a factor of 3 larger.

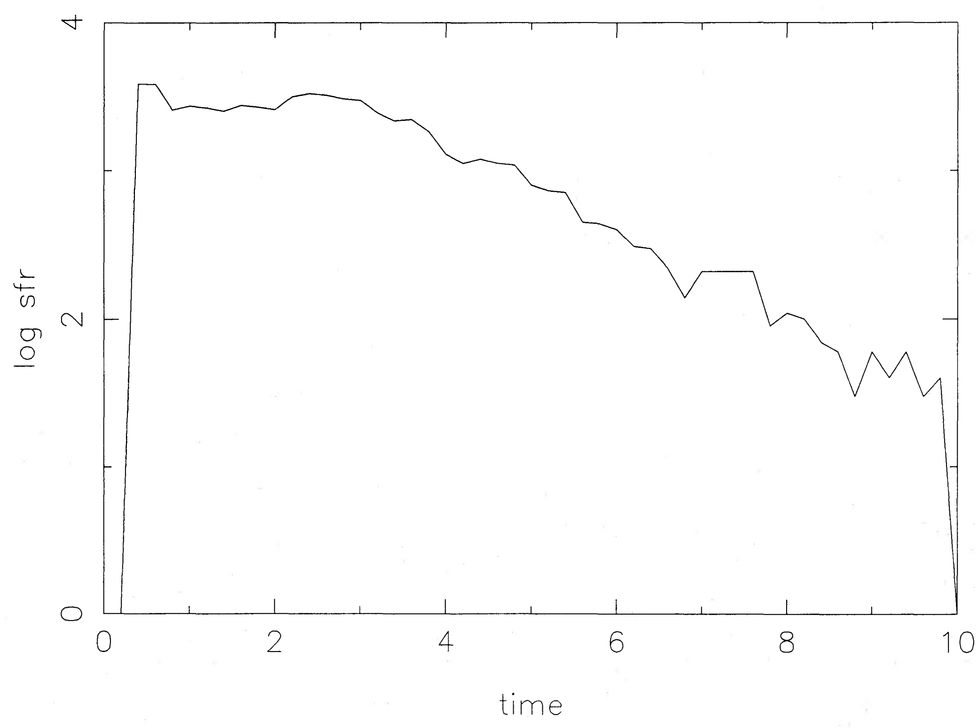

FIG. 5.—The logarithm of the star formation rate vs. time for the cluster model, measured in particles per unit time. The initial bump in the star formation rate comes from particles placed very near together in the initial random distribution falling together to make stars. The drop around time 4 is a result of the exhaustion and removal of the remaining gas in the galaxies. From time 4 to time 10 the SFR declines approximately exponentially, with an e-folding time of 1.6 units.

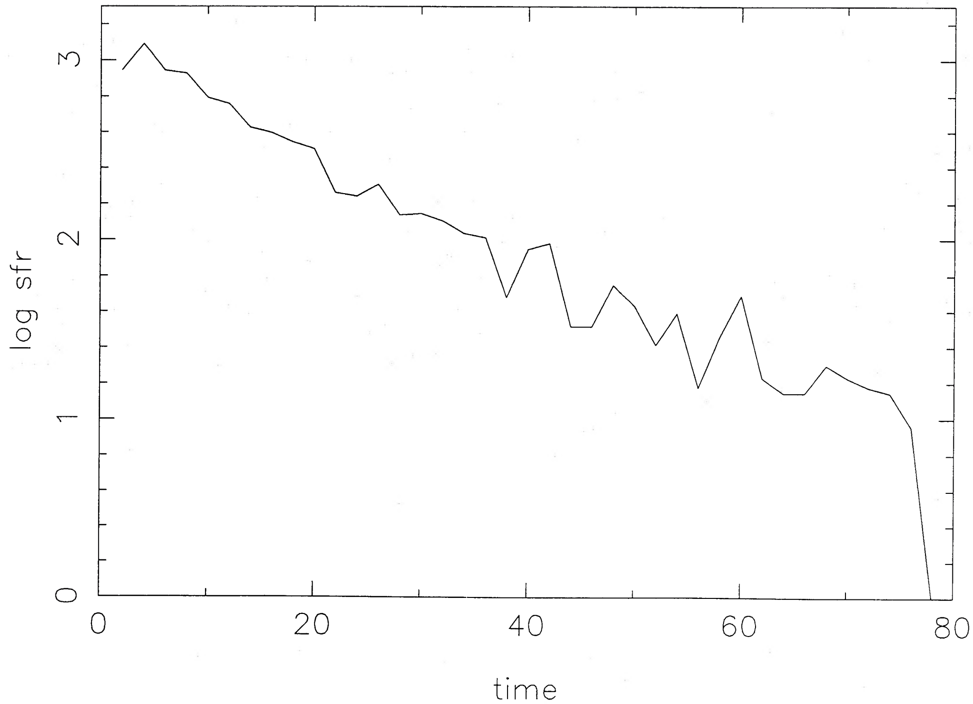

FIG. 6.—The logarithm of the star formation rate in the $\Omega = 1$ model. The SFR declines approximately exponentially, with an e-folding time of 12.4 units, much more slowly than in the cluster model. The current epoch is identified as 35.8 time units.

logarithm of the star formation rate is plotted against time. In both cases, after an initial period of rapid star formation the star formation rates are best fitted by an exponential in time. A power law does not provide as satisfactory a fit over a wide a range of the data as the exponential. The e-folding times for the decay of star formation are 1.6 time units for the cluster model, and 12.4 time units for the $\Omega = 1$ model.

It is no surprise in the cluster model that a characteristic time scale of the order 3 units appears, since this is a characteristic time, maximum expansion. As the cluster grows the velocity dispersion rises sufficiently that the virialized gas in the cluster cannot cool, and the remnant low density gas in the halos is swept out of the galaxies by the pressure of the cluster gas. The remaining dense gas within the stellar galaxies is consumed in a final stage of star formation. It appears that galaxies fairly quickly turn the gas in the bottom of a potential well into stars, but continuing infall of gas, and mergers with gas rich galaxies, continue to power the star formation process. Consequently star formation here is spread over a time comparable to the dynamical time of a small group of galaxies (Baron and White 1987). The adopted scaling of 51 km s^{-1} per grid unit, 40 kpc per velocity unit, implies a time unit of 7.8×10^8 yr. The period of most intense star formation in this cluster model lasts ~ 4 time units, or 3×10^9 years. The exponential time scale of the decay of star formation, 1.6 units, scales to 1.2×10^9 yr. This might be interpreted as the way that gas poor E and S0 galaxies originate (Larson, Tinsley, and Caldwell 1980; Sancisi 1983; Carlberg 1987).

In the $\Omega = 1$ model there is no intrinsic characteristic time scale of the dynamics of the clustering. The exponential decay of star formation seen in Figure 6 strongly suggests that star formation works from an effectively finite and fixed initial reservoir of gas that can be processed into gas at a fixed rate proportional to the remaining gas available. The time scale of the decay of star formation, 12.4 units, is $\sim 35\%$ of the age of the model (35.8 units) at the current epoch. This time variation is similar to that favored in the "μ-models" of Bruzual (1983). Most galaxies "form" between a redshift of 2 and 3 in this experiment, which may be uncomfortably low, but they are mostly small objects that later merge to build up big galaxies, and therefore may be difficult to detect (Baron and White 1987). The formation of new galaxies, except for mergers, is essentially finished at a redshift of 1. At lower redshift star formation remains active, but is decaying with an e-folding time scale of 5 Gyr.

An important implication of the variation of the rate of star formation with time is that galaxy formation depends very strongly on the environment, in a combination of accretion, merging, and stripping (Gott and Gunn 1972; Toomre 1977; Gunn 1977; Frenk *et al.* 1987; Baron and White 1987; Ryden and Gunn 1987). That is, most galaxies begin as chaotic structures that fall together in an initial collapse, followed by a long period of accretion of surrounding gas lumps and small companion galaxies. This buildup of galaxies is essentially terminated once a substantial group forms, since the probability of merging collisions is low, and remnant internal gas is removed from the galaxies by sweeping.

d) Luminosity Functions and Mergers

The luminosity function of the galaxies in the cluster model is shown at two times, $t = 4.39$ and $t = 10.39$ in Figure 7. Compared to Paper I there is somewhat less tidal shredding, and no exceptionally massive cD galaxy has formed in the center of the cluster. The galaxies in Paper I were on the average 25%–50% larger, depending on the particular time chosen for comparison, thus they were relatively more vulnerable to tides and mergers. The luminosity function varies little until the time of maximum expansion when the galaxies start

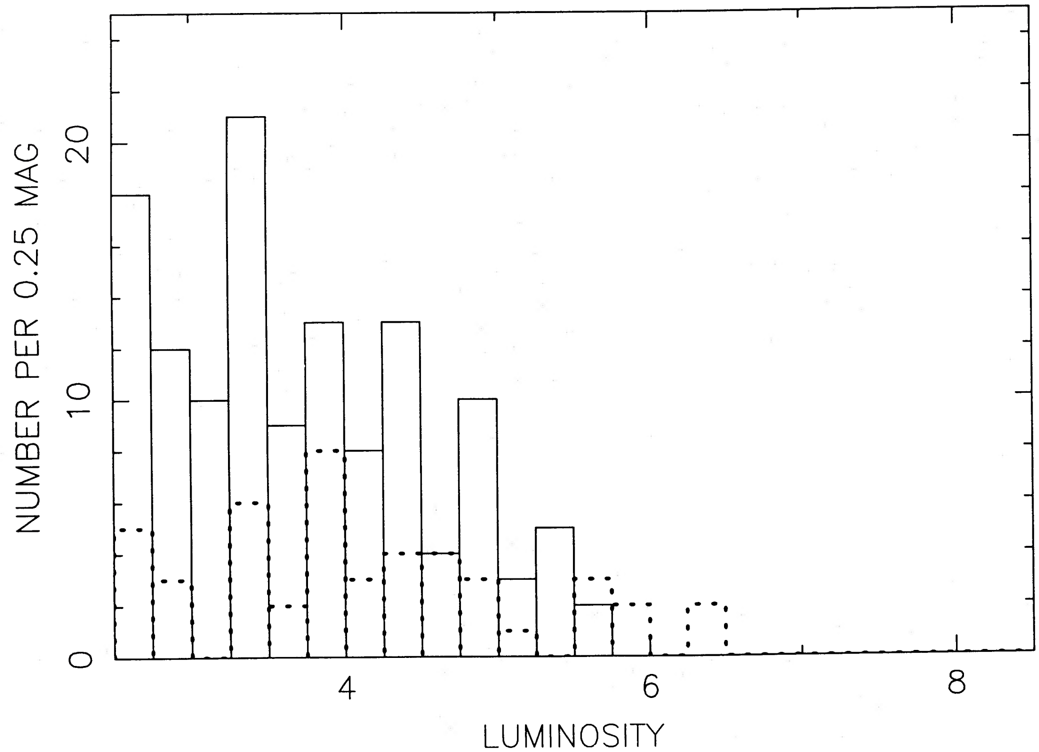

FIG. 7.—The luminosity function of the galaxies in the $\Omega_i = 5/3$ cluster model at times 4.39 and 10.39, where luminosity is calculated as 2.5 log N, with N being the number of particles in the galaxy.

being drawn into the cluster. Table 2 shows that the numbers of galaxies is reduced, through mergers and tidal disruption, as the cluster forms. The numbers of galaxies are reduced nearly by a factor of 3, with their mean mass going up by 50%. The fact that no extremely large galaxy forms here, even though exactly the same initial conditions as in Paper I were used, emphasizes that the fate of galaxies in any particular cluster are strongly dependent on their detailed circumstances (Richstone and Malamuth 1983).

The luminosity function of the $\Omega = 1$ model, shown in Figure 8, appears to evolve considerably more at the high-luminosity end than the cluster model. That is, mergers never really stop in this model, a consequence of the absence of groups containing significant numbers of galaxies and quite likely connected to the relatively large size of the galaxies, of order $50h^{-1}$ kpc. During the late part of the experiment the correlation function evolves relatively little, whereas the luminosity function is building up more high-mass galaxies. The lower mass galaxies remain nearly constant in number, especially in comparison to the cluster model, a consequence of the diminished importance of tidal shredding in the generally weaker clustering environment of this model.

The origin and fate of stars within galaxies are summarized in Table 2. The collumns show (1) the model time, (2) the cumulative number of stars formed, (3) the percentage of these stars within galaxies containing at least 10 stars, (4) the total

TABLE 2

GALAXY FORMATION

Time (1)	Star Particles (2)	Percentage Stars in Galaxies (3)	Number of Galaxies (4)	Percentage New Stars (5)	Percentage Galactic Stars (6)	$\bar{m}$ Galaxy (7)	Number of Merger Remnants (8)	$\bar{m}_{mg}$ (9)
				$\Omega_i = 5/3$				
2.39	5770	34	106	100	0	18.7	0	0
4.39	10578	51	128	66	22	41.6	6	125
6.39	12050	42	103	22	69	48.5	8	153
8.39	12412	33	71	8	81	57.1	5	167
10.39	12508	26	46	2	84	70.6	2	360
				$\Omega = 1$				
5.96	4584	10	37	100	0	11.7	0	0
18.3	12454	54	238	63	6	28.1	3	98
35.8	16546	64	243	30	57	43.7	30	153
55.0	18450	66	214	14	77	57.4	26	241
81.3	19286	66	176	6	85	72.5	17	301

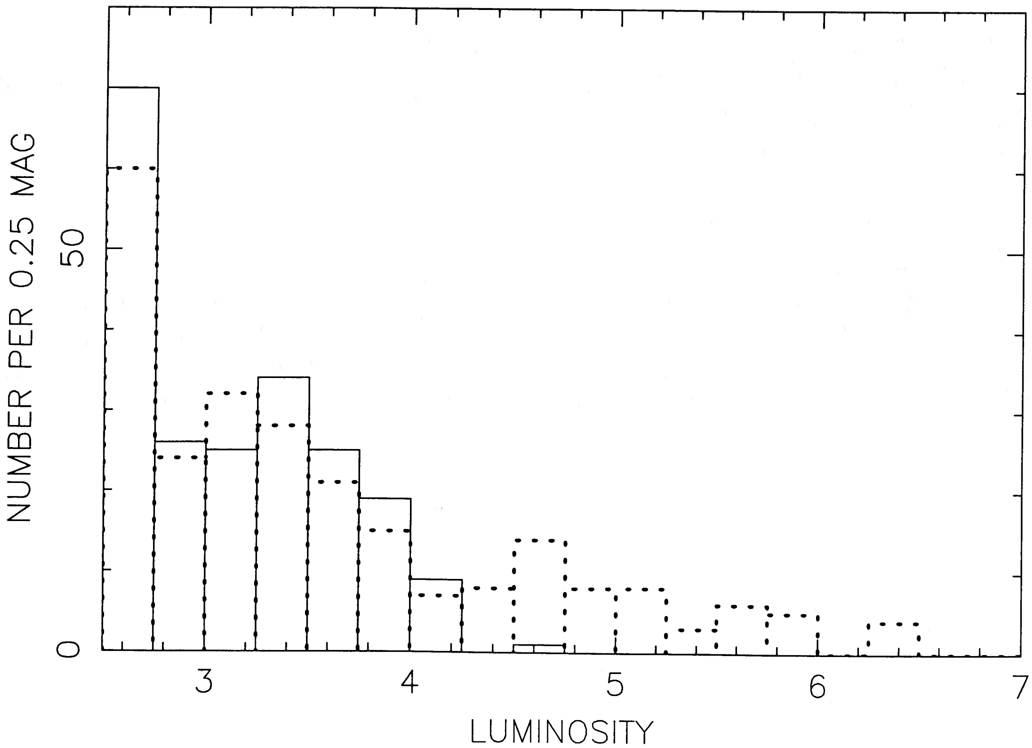

FIG. 8.—The luminosity function of the galaxies in the $\Omega = 1$ models at times 12.3 and 35.8. The luminosity is 2.5 log N, with N being the number of particles in the galaxy.

number of these galaxies, (5) the percentage of the stars in the galaxies that were formed in the time interval from the previous line in the table, (6) the percentage of the stars in galaxies that were previously in the same galaxy, and (7) the mean mass of the galaxies. The fraction of the stars that stay in galaxies is quite different in the two experiments. The $\Omega = 1$ experiment maintains a nearly constant fraction of two-thirds of all stars in galaxies (the rest lingering near the "edges" of the galaxies), whereas the cluster experiment rises to a maximum of 51% stars in galaxies and then declines, as tidal fields strip stars off the edges of the galaxies.

The rate of merging between galaxies to build new, larger galaxies is of considerable interest. A merger is counted when a galaxy contains some large percentage of the stars from each of at least two preexisting galaxies. The number of mergers is not sensitive to the value chosen for the percentage of merged stars, the number of merger remnants in the $\Omega = 1$ experiment dropping from 30 down to 21 as the percentage is raised from 30% to 80%. In Table 2 column (8) shows the number of galaxies that can be identified as merger remnants, and column (9) shows the mean mass of the merger remnants. Mergers give rise to galaxies that are typically 3–4 times heavier than an average galaxy, and 10%–15% of all galaxies are merger remnants, rather remarkably similar to Toomre's (1977) estimated fraction. The ratio of the average masses of merged to unmerged galaxies is consistent with the hypothesis that merged galaxies are elliptical and S0's, since they tend to be more massive than spirals (Sandage, Binggeli, and Tammann 1985). Furthermore, if the Hubble sequence is a mass sequence, then the observation that ellipticals are more strongly correlated than spirals (Davis and Geller 1976; Giovanelli, Haynes, and Chincarini 1986) is completely consistent with the same finding in this model; see Figures 9 and 10. Because the galaxies here are rather too large and heavy to be average galaxies this measured rate is likely an overestimate, but since merger dynamics is likely dominated by the extended dark halos of galaxies, this estimate may not be too far off. In any case, this estimate of the rate of mergers should be regarded as preliminary.

An interesting point related to merging is the fractional mass gain for an average galaxy over a redshift interval comparable to that used in the Loh and Spillar (1987) redshift volume test. Although the number of galaxies changes relatively little from $z = 0.56$ ($t = 18.3$) to $z = 0$, the mean galactic mass increases considerably, leading to an error in the Loh and Spillar Ω estimate through an incorrect estimate of the normalizing constant of the luminosity function. Bahcall and Tremaine (1988) estimate that the mass gained for an L_* galaxy is 30% from a redshift of 0.75, likely a conservative estimate since they calculated infall based on dynamical friction on circular orbits. Here, Table 2 shows that from a redshift of 0.56 the average galaxy gains 36% of its mass. Once again, the agreement between the two figures is encouraging but awaits much larger N experiments for confirmation.

Overall, the importance of mergers at low redshifts is considerably larger in this experiment than in the work of Aarseth and Fall (1980). There are two differences from their simulations that enhance the merger rate. Most importantly, the galaxies here have extended dark halos that increase the merger cross section. And second, the galaxies here have a second route for gaining mass: the conversion of gas to stars.

IV. CORRELATION FUNCTIONS AND MERGERS

The tendency for galaxies to be more strongly correlated than the dark matter, or the remaining gas, was an important result in Paper I (and see White *et al.* 1987). The correlation

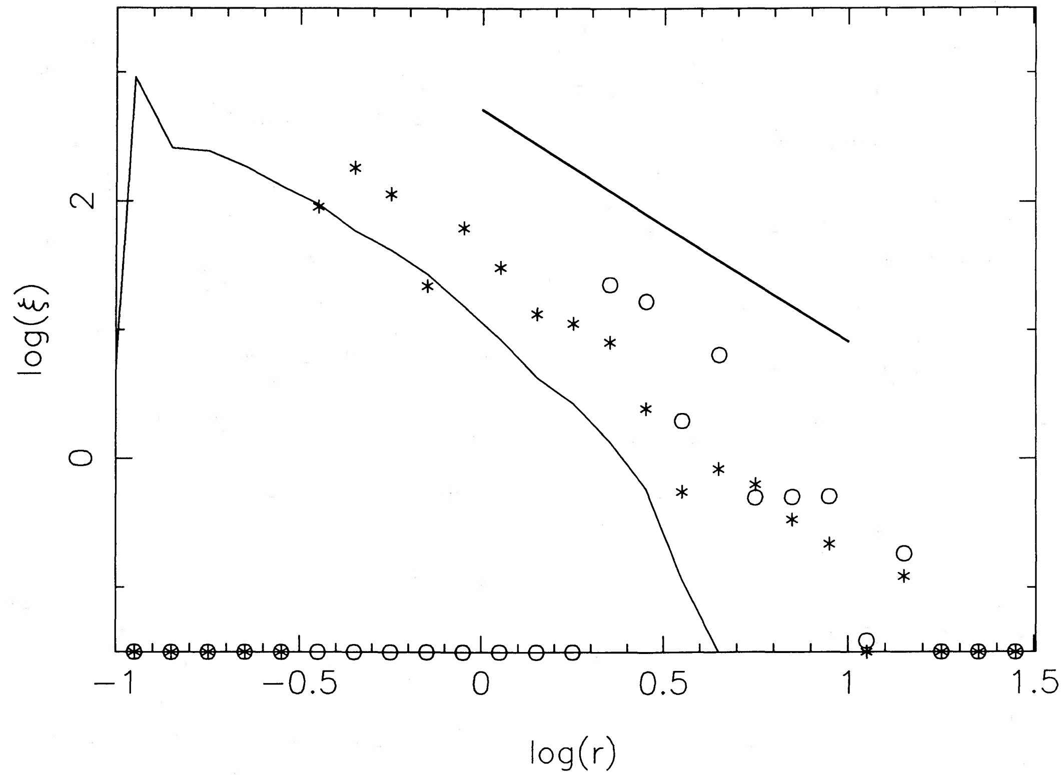

FIG. 9.—The correlation function at time 12.26 of the dark matter (*solid line*), all galaxies containing more than 10 particles (*stars*), and all galaxies containing more than 20 particles (*open circles*)

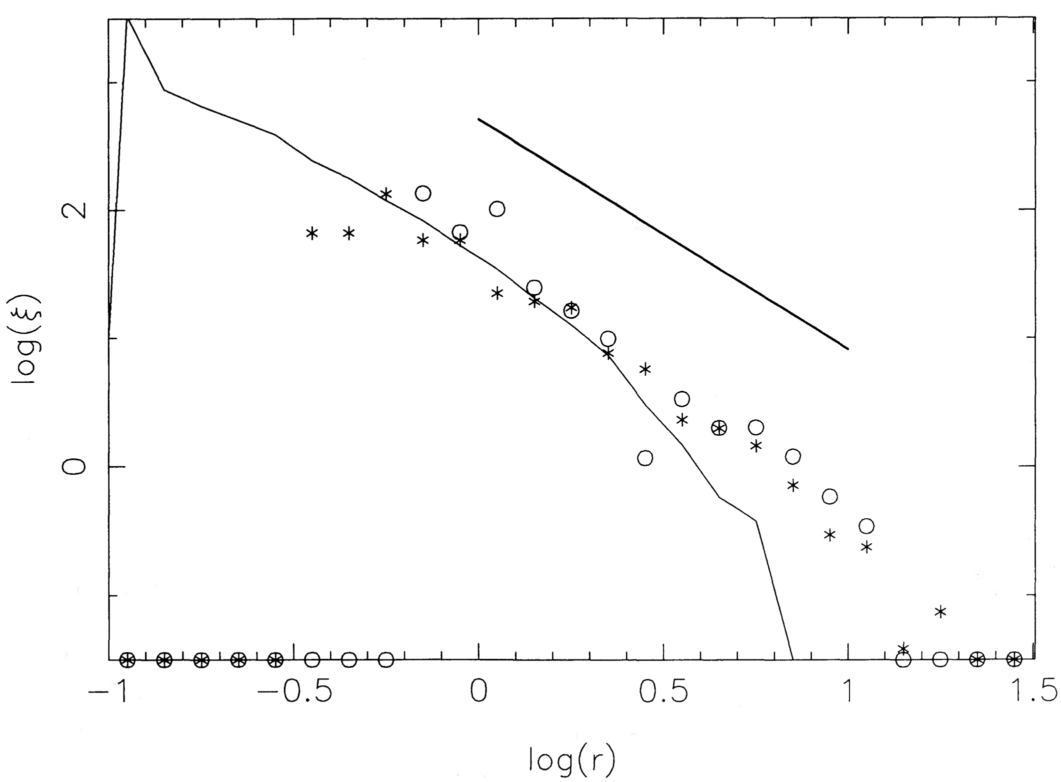

FIG. 10.—The correlation function at time 35.8 of the dark matter (*solid line*), all galaxies containing more than 10 particles (*stars*), and all galaxies containing more than 30 particles (*open circles*).

functions of the galaxies and dark matter in the $\Omega = 1$ experiment when the galaxies have nicely formed, time $t = 12.2$ ($z = 1.04$) are shown in Figures 9 and 10, and the time that is identified as the current epoch, $t = 35.8$, are shown, in comoving coordinates. At a redshift near 1 the galaxy correlation function has an amplitude typically 3 times higher than the dark matter. The galaxy $\xi(r)$ is more nearly a power law than the dark matter. As the experiment expands to the time identified as the current epoch the bias is greatly reduced.

Relatively less evolution of the galaxy correlation function than of the dark matter correlation function is expected, since the galaxies form close to potential maxima, and hence on the average have lower than average infall velocities (e.g., Bond and Couchman 1987). In the case of stable clustering the amplitude of the correlation function declines as $(1 + z)^3$, a factor of 8 to a redshift of 1, whereas the evolution observed in the galaxies here is approximately a factor of 2 less. There is some weak observational evidence that the amplitude of the correlation function at a redshift near 1 is higher than expected for $(1 + z)^3$ evolution (Koo and Szalay 1984; Pritchet and Infante 1986).

The relation between the peaks in the initial density field and the mass of the galaxies is shown in Figures 11 and 12. The initial fluctuation field needs to be filtered on an appropriate length scale to eliminate subgalactic peaks. A procedure similar to that of Barnes and Efstathiou (1987) is adopted. The initial particle positions are interpolated onto a 64^3 grid, then Gaussian filtered, using a half width $64/6 = 10.3$ grid units. The mass containing this radius is nearly equal to the average mass of the galaxies, using the measured formation efficiency of 0.04. The filter gives 260 local maxima, as found by comparing the filtered density field at the grid points to the surrounding 26 grid points. The variation, σ_ρ, of the filtered density field is measured, and used to define $\nu = (\Delta\rho/\rho)/\sigma_\rho$. A plot of the normalized overdensity versus mass in plotted at two times, 12.2 and 35.8, the same as the two displayed correlation functions.

The plots show that there is very little correlation of mass and overdensity when the galaxies form, except that galaxies form from positive overdensity regions. Later there is a fairly clear trend of increasing overdensity with mass. The heaviest galaxies are mostly the result of merging two preexisting galaxies. Evidently the highest peaks are the ones most likely to merge to make heavier galaxies. Conversely, galaxies that form in low overdensity peaks are relatively unlikely to merge.

V. CLUSTER CONTENTS

a) *Loose Stars*

Figure 13 shows the radially averaged cluster density profile of all types of particles not in galaxies, that is, dark matter, gas, and stars not linked to galaxies at $t = 10.39$ in the cluster experiment. The number of loose stars is dependent upon the link length only in the center of the cluster, as shown by lines for galaxies defined by two linking parameters. There are nearly as many loose stars spread around in the cluster as stars in galaxies. The presence of a significant (10%–50%) stellar component unbound from galaxies has been discussed at length in various models of cluster formation and evolution (e.g., Malamuth and Richstone 1983; Merritt 1984) and likely detected in the Coma cluster (de Vaucouleurs and de Vaucouleurs 1970; Melnick, White, and Hoessel 1977; Thuan and Kormendy 1977) and other clusters (Oemler 1973).

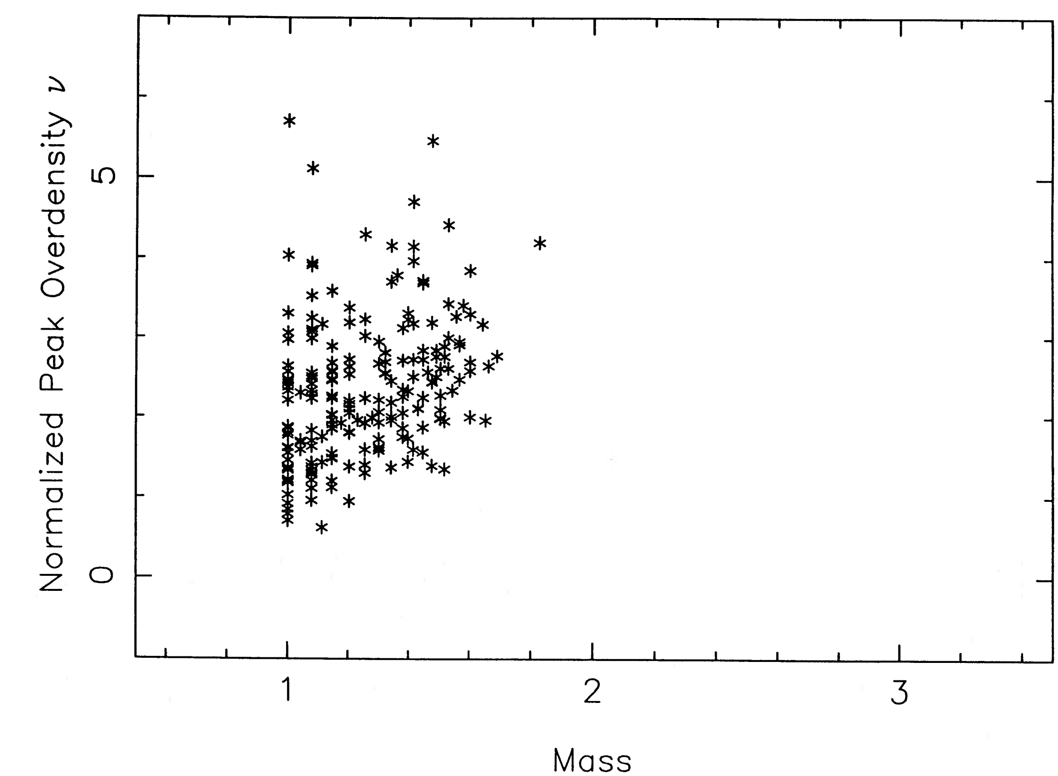

FIG. 11.—Peak overdensity in identified galaxies (groups of at least 10 particles each having a separation to its nearest neighbor no more than 0.1 of the average separation) vs. the mass of the galaxy, measured at time 12.26

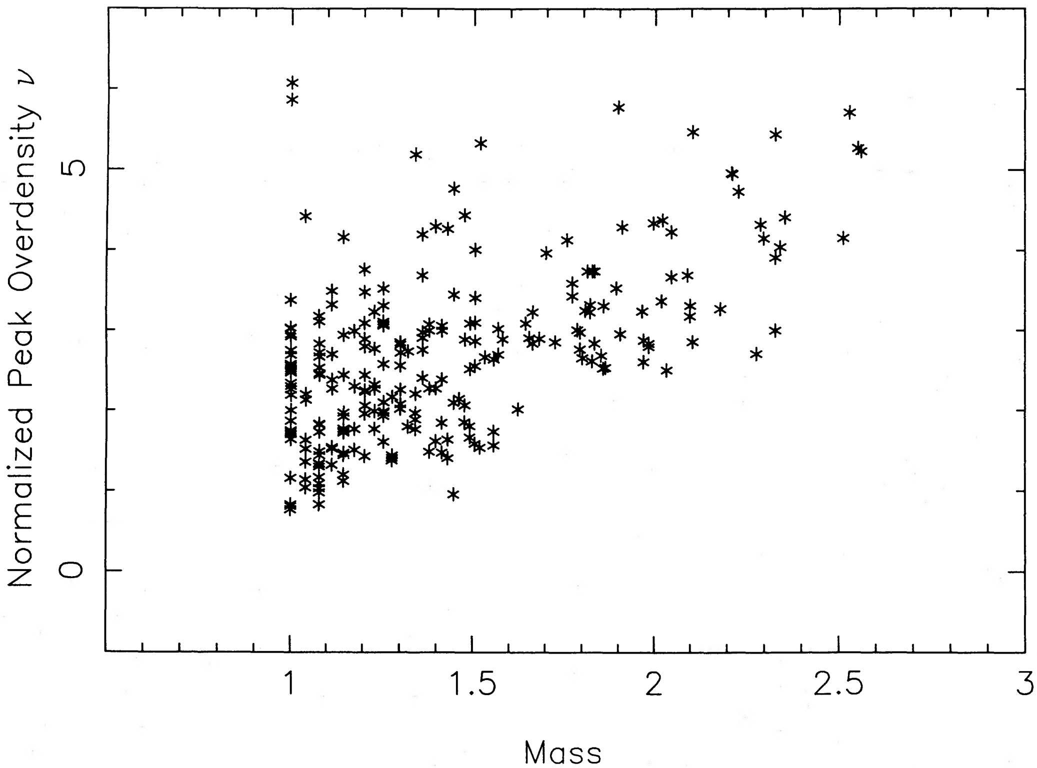

FIG. 12.—Peak overdensity in galaxies identified at time 35.8. Comparison with Fig. 10 suggests that the trend of peak overdensity with mass arises from mergers preferentially joining galaxies having high initial overdensities.

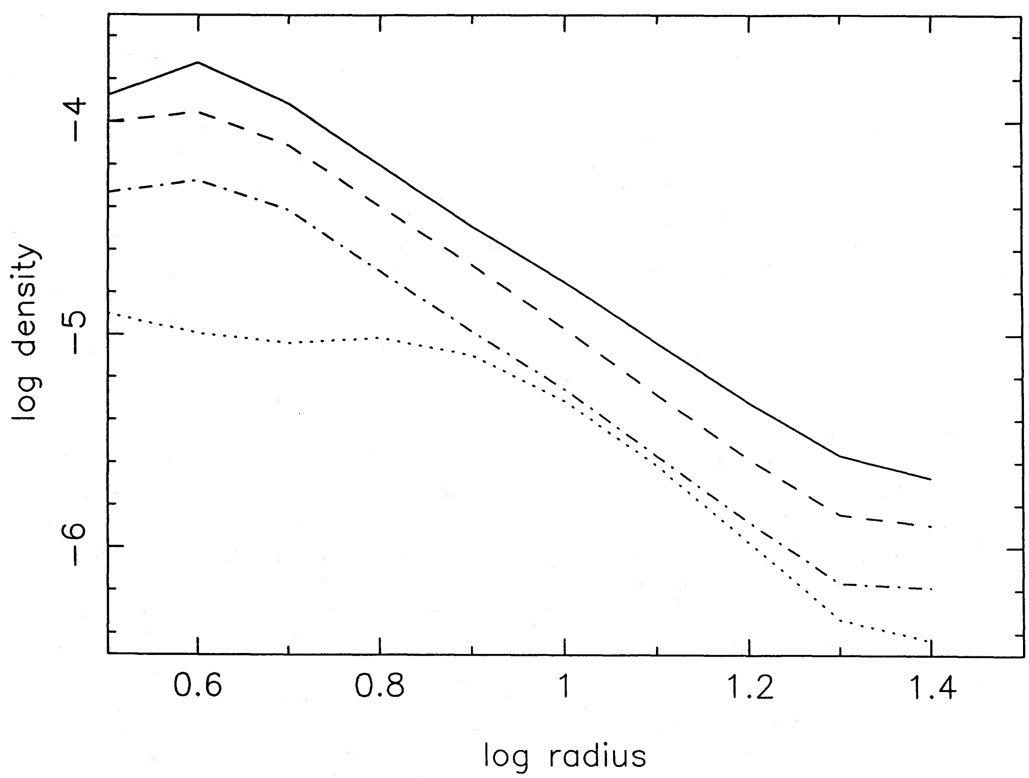

FIG. 13.—Radial volume density profiles of the dark matter (*solid line*) gas (*dashed line*) and unbound stars. Dotted line links stars with separations up to 0.5 grid units to galaxies, and dot-dashed line uses the standard link length of 0.2 grid units to link particles into galaxies. All densities are normalized to the total number of particles, 65,536. The peak *projected* stellar density is 9.8 particles per square unit.

In the group of galaxies that forms here the average surface density of loose stars in the cluster is near to 1 particle per square unit. The average galaxy composed of 71 particles with a half mass radius of 0.23 units for an average surface density of 427 particles per square unit, whereas the cluster background light peaks in the core at 9.8 particles per square unit, or 4.1 mag fainter. If the average surface brightness of a galaxy is ~ 23.0 mag arcsec^{-2} then the predicted background light in the group would be ~ 27 mag arcsec^{-2} at the cluster center. It is encouraging that such light has probably been detected in Coma, although one would think that smaller more compact groups would be more likely sites for such light, since tides tend to diminish in importance in larger objects, so that a fixed amount of light would be spread over a growing volume. The background light found here is likely somewhat of an overestimate, since some of the stars formed early on more or less at random, and the tightness of the galaxies depends on the star formation parameter d_*, which could easily be made a little smaller so that the galaxies are more compact and less stripping occurs. These corrections would likely reduce the number of loose stars by a factor of 2 or so. In that case the background light should be ~ 5 mag below the average galaxy surface brightness.

b) *Gas in the Cluster*

The efficiency for forming stars from the gas in both models is $\sim \frac{1}{3}$, in the cluster model leaving 20,260 gas particles behind, out of an initial 32,768. The maximum cool gas fraction in galaxies is 10% of the total baryonic mass. The cluster of galaxies present at the end of the simulation contains nearly 3 times as much baryonic mass in hot cluster gas as in galaxies, a situation that appears to prevail in observed clusters of galaxies (for a review see Sarazin 1986). A point of caution is that most of the well-observed clusters are large clusters, with a velocity dispersion near 1000 km s^{-1}, whereas this group has a velocity dispersion that scales to 500 km s^{-1}. The best studied groups are large, and therefore may have somewhat different X-ray properties than the group of galaxies found here.

The spatial distribution of the hot gas is always smoother than the underlying dark matter distribution, as shown in Figure 1. A faint numerical worry is that this smoothness may be a consequence of excessive diffusion in the current gas code, but on the face of it, the possibility seems unlikely. The diffusion time scale over a distance R is $t_d \approx R^2/(l\sigma)$, where l is the mean free path, and σ is the random velocity. The time to diffuse from the center to the half mass radius, $R = 7$, at a mean density of 5 units and $\sigma = 10$, is $t_d = 10.7$ units of time. As a check, the path of a few gas particles were followed in detail, and they appear to move relatively little in radius once the cluster forms, the radial diffusion being of order 1 unit of distance, roughly in accord with the above formula.

The cluster gas in the model has an equivalent temperature that is nearly independent of radius, closely following the dark matter velocity dispersion. Diffusion could act to falsely remove temperature gradients, but as argued above the diffusion time scale should be longer than the cluster lifetime. Some models for the X-ray emission from the Coma cluster, suggest that the temperature peaks toward the center of the cluster, (Cowie, Henriksen, and Mushotsky 1987; The and White 1988) although the very rich Coma cluster is not directly comparable to the small cluster here, but this may be a consequence of heat addition by processes not modeled here. The scaled temperature of the model cluster is ~ 2.5 keV, considerably lower than the range of temperatures appropriate to Coma. Poor cD clusters have temperatures of 1–2.5 keV, and appear to be overall quite a good match to the properties of this cluster (Biermann, Kronberg, and Madore 1982; Kriss, Cioffi, and Canizares 1983). The brightest galaxy in the group here contains only 3% of the galactic cluster light making this group fairly normal, rather than a good candidate for cD status.

The main conclusions of this section is that the cluster gas is a good tracer of the cluster dark matter, although it is somewhat more smoothly distributed and that both have a nearly isothermal temperature distribution in this model.

VI. CONCLUSIONS

A simple numerical algorithm that allows gas and star formation to be included in a cosmological N-body model is introduced in this paper. The results of two galaxy formation experiments are presented, one mimicking the formation of a small cluster in a background having $\Omega_i = 5/3$, and for comparison, an experiment with $\Omega = 1$. The cooling and star formation rates are based on a parametrization of the radiative cooling curve. The resulting galaxies are certainly not completely identical to the galaxies in the universe, but the many points of similarity suggest that this model is useful for investigations of the relation between cosmological quantities and galaxy properties. The experiments emphasize that galaxy formation is not sharply peaked in time, but is an ongoing process through mergers and accretion, whose rate depends on the clustering environment. In the $\Omega = 1$ model, galaxy formation takes place between a redshift of 2 and 3 mostly as small objects that later increase in mass. The increase in the number density of galaxies ceases at a redshift of one. Thereafter mergers occur preferentially between galaxies that can be identified as arising from the highest initial density fluctuations, that help to build increase the correlation between mass and clustering length. As a result of merging and accretion in the $\Omega = 1$ model an average galaxy increases its mass 36% from a redshift of 0.56 to the present, although only 30 out of 243 galaxies can be clearly identified as merger remnants. These conclusions are compromised to some degree by the relatively few particles per galaxy, and the relatively large softening required for the simulation.

Between 30%–50% of the gas turns into stars, with about two-thirds of the stars being contained in galaxies in the general clustering environment of the $\Omega = 1$ model. In the cluster model the galaxies are severely eroded by tidal stripping, reducing the number of galaxies by a factor of 2 and leaving a background distribution of loose stars with a predicted surface brightness in the core of 27–28 mag arcsec^{-2}.

Star formation terminates quickly once the cluster gas density and velocity dispersion rise sufficiently that accretion is shut off and the remaining gas in the galaxies is swept away. On the other hand, galaxies in less dense environments continue to form stars, although the rate of star formation decays approximately exponentially in time, with a time constant comparable to the current Hubble time. The presence of the exponential form in both cases suggests that galaxies do form with a fixed reservoir of gas that can be tapped to build up the galaxy. The reservoir can be severely depleted by stripping in dense environments like a group or cluster.

The cluster that forms in the $\Omega_i = 5/3$ model contains hot gas, loose stars, and dark matter. The model probably overestimates the number of loose stars, but even a conservative estimate suggests that the group should contain a luminosity in loose stars comparable to that contained in the galaxies. The hot gas in the cluster is almost exactly isothermal, at a temperature that scales to 2.5 keV, and is identical to the random velocities in the dark matter. The gas is always spread more smoothly than the dark matter. Although there is a possibility that this is a consequence of an excessive diffusion of the gas, it does imply that X-ray luminosity may give an excessively smooth impression of the potential in a cluster.

The distribution of the galaxies clearly reflects the initial density fluctuations, and galaxies form with an enhanced clustering with respect to the dark matter. The excess of the galaxy correlation function over that of the underlying dark matter begins as nearly a factor of 5, but the dark matter catches up (in this model) to be nearly equal at late times. Massive galaxies tend to be somewhat more strongly clustered than light ones, a consequence of the enhanced merging of protogalaxies that form from relatively high peaks.

The main limitation of the current experiments is the relatively few particles that were used, restricting the dynamic range of the experiments, and interfering with the spectrum of fluctuations through the white noise of the particle distribution. Galaxy formation should depend to some significant degree on the details of the cosmology and depend significantly on the ability to properly resolve gravity on the scales of galaxies. Therefore the experiments presented here should be viewed as indicative of the qualitative results that can be expected, but quantitative details await experiments for a specific cosmological model, with more particles.

This work was supported by a grant from the NSERC of Canada and a grant of time from the Pittsburgh Supercomputer Center. I thank the University of Michigan for its hospitality, and CITA for a Reinhardt fellowship.

REFERENCES

Aarseth, S. J., and Fall, S. M. 1980, *Ap. J.*, **236**, 43.
Bahcall, S., and Tremaine, S. D. 1988, *Ap. J. (Letters)*, **326**, L1.
Barnes, J., and Efstathiou, G. 1987, *Ap. J.*, **319**, 575.
Baron, E., and White, S. D. M. 1987, *Ap. J.*, **322**, 585.
Bean, A. J., Efstathiou, G., Ellis, R. S., Peterson, B. A., and Shanks, T. 1983, *M.N.R.A.S.*, **205**, 605.
Biermann, P., Kronberg, P. P., and Madore, B. F. 1982, *Ap. J. (Letters)*, **256**, L37.
Bond, J. R., and Couchman, H. M. P. 1987, *preprint*.
Blumenthal, G. R., Faber, S. M., Primack, J., and Rees, M. J. 1984, *Nature*, **311**, 517.
Bruzual, G. 1983, *Ap. J.*, **273**, 105.
Carlberg, R. G. 1987, *Elliptical Galaxies, IAU Symposium 127*, ed. T. de Zeeuw (Dordrecht: Reidel), p. 353.
———. 1988, *Ap. J.*, **324**, 664 (Paper I).
Cowie, L. L., Henriksen, M., and Mushotsky, R. 1987, *Ap. J.*, **317**, 593.
Davis, M., and Geller, M. H. 1976, *Ap. J.*, **208**, 13.
Davis, M., and Peebles, P. J. E. 1983, *Ap. J.*, **267**, 465.
de Vaucouleurs, G., and de Vaucouleurs, A. 1970, *Ap. Letters*, **5**, 219.
Fitchett, M., and Webster, R. 1987, *Ap. J.*, **217**, 653.
Frenk, C. S., White, S. D. M., Efstathiou, G., and Davis, M. 1985, *Nature*, **317**, 595.
Giovanelli, R., Haynes, M. P., and Chincarini, G. L. 1986, *Ap. J.*, **300**, 77.
Gott, J. R., and Gunn, J. 1972, *Ap. J.*, **176**, 1.
Gunn, J. 1977, *Ap. J.*, **218**, 592.
Huchra, J. P., and Geller, M. J. 1982, *Ap. J.*, **257**, 423.
Kriss, G. A., Cioffi, D. F., and Canizares, C. R. 1983, *Ap. J.*, **272**, 449.
Koo, D. C., and Szalay, A. S. 1984, *Ap. J.*, **282**, 390.
Larson, R. B., Tinsley, B., and Caldwell, N. 1980, *Ap. J.*, **237**, 693.
Loh, E. D., and Spillar, E. J. 1987, *Ap. J. (Letters)*, **307**, L1.
Malamuth, E. M., and Richstone, D. O. 1984, *Ap. J.*, **276**, 413.
Melnick, J., White, S. D. M., and Hoessel, J. 1977, *M.N.R.A.S.*, **180**, 207.
Merritt, D. 1984, *Ap. J.*, **276**, 26.
Oemler, A. 1973, *Ap. J.*, **180**, 11.
Prichet, C. J., and Infante, L. 1986, *A.J.*, **91**, 1.
Raymond, J. C., Cox, D. P., and Smith, B. W. 1976, *Ap. J. (Letters)*, **204**, L290.
Rees, M. J., and Ostriker, J. P. 1977, *M.N.R.A.S.*, **179**, 451.
Richstone, D. O., and Malamuth, E. M. 1983, *Ap. J.*, **268**, 30.
Ryden, B. S., and Gunn, J. E. 1987, *Ap. J.*, **318**, 15.
Sancisi, R. 1983, in *IAU Symposium 100, Internal Dynamics and Kinematics of Galaxies*, ed. E. Athanassoula (Dordrecht: Reidel), p. 55.
Sandage, A., Binggeli, B., and Tammann, G. A. 1985, *A.J.*, **90**, 1759.
Sarazin, C. 1986, *Rev. Mod. Phys.*, **58**, 1.
Silk, J. 1977, *Ap. J.*, **211**, 638.
The, L. S., and White S. D. M. 1988, *A.J.*, **95**, 15.
Thuan, T. X., and Kormendy, J. 1977, *Pub. Astr. Soc. Pacific*, **89**, 466.
Toomre, A. 1977, in *Evolution of Galaxies and Stellar Populations*, ed. B. M. Tinsley and R. B. Larson (Yale Observatory: New Haven), p. 401.
White, S. D. M., Davis, M., Efstathiou, G., and Frenk, C. S. 1986, *Nature*, **330**, 451.

R. G. Carlberg: Department of Astronomy, University of Toronto, Toronto, Ontario M5S 1A1, Canada